Shape Control in Epitaxial Electrodeposition: Cu_2O Nanocubes on InP(001)

Run Liu,[†] Fumiyasu Oba,[‡] Eric W. Bohannan,[†] Frank Ernst,[‡] and Jay A. Switzer*[,†]

Department of Chemistry and Graduate Center for Materials Research, University of Missouri−Rolla, Rolla, Missouri 65409-1170, and Department of Materials Science and Engineering, Case Western Reserve University, 10900 Euclid Avenue, Cleveland, Ohio 44106-7204

Received August 30, 2003
Revised Manuscript Received November 11, 2003

Introduction. Regular arrays of epitaxial semiconductor nanocrystals on semiconductor substrates are of interest for a variety of applications, such as optical electronic devices, quantum computing, and information storage.[1] One means of obtaining such structures is to produce self-assembled islands by strain relief during epitaxial growth, as in the vapor deposition of InAs on GaAs[2] or Ge on Si.[3−5] Chemists have demonstrated that colloidal nanocrystals with monodispersed size and varied shapes can be obtained from solutions by the use of surfactants and by the precise control of the growth conditions.[6−10] Electrodeposition has also been shown to be well-suited to grow nanostructures.[11] A unique feature of electrodeposition is the ability to tune the orientation and morphology of electrodeposited films by controlling the solution pH or the electrode overpotential.[12] These degrees of freedom are not available in vapor deposition. We have previously used electrodeposition in aqueous solution to form epitaxial films of δ-Bi_2O_3,[13] Cu_2O,[14] ZnO,[15] and Fe_3O_4[16,17] on gold single crystals and epitaxial Cu_2O[18] films on silicon single crystals. Lincot et al. have electrodeposited epitaxial films of CdTe on InP(111)[19] and ZnO on GaN(0002).[20] Recently, we have shown that it is possible to deposit epitaxial bulk Cu_2O films onto InP(001) with tunable morphologies[21] and epitaxial chiral CuO films onto Au single crystals.[22] Here, we extend this work to the electrodeposition of epitaxial Cu_2O nanocrystals onto InP(001). The shape of the nanocrystals can be selected by controlling the solution pH and varied from nanopyramids at pH 9 to nanocubes at pH 12.

Cuprous oxide (Cu_2O) is a p-type semiconductor that has potential application in solar energy conversion and catalysis.[23] There is also evidence that Bose-Einstein condensation of excitons can occur when Cu_2O is irradiated with highly intense light.[24,25] Single-crystalline Cu_2O nanocubes would be expected to spatially confine excitons and effectively increase their concentration. Moreover, the Cu_2O/InP heteroepitaxial system is interesting because of its large lattice mismatch of −27.2%.

Experimental Section. Electrochemical experiments were carried out using an EG&G Princeton Applied Research (PAR) model 273A potentiostat/galvanostat. The deposition was performed in a three-electrode cell with a platinum wire as the counter electrode and a saturated calomel electrode (SCE) as the reference electrode. The deposition solutions were 0.4 M $CuSO_4$ and 3 M lactic acid at pH 9 and pH 12. The deposition temperatures were 65 °C at pH 9 and 25 °C at pH 12. The applied potentials were −0.20 V vs SCE at pH 9 and −0.34 V vs SCE at pH 12.

The n-InP(001) wafers were supplied by Wafer Technology Ltd., doped with sulfur to a resistivity of approximately 1.6×10^{-3} Ω-cm, corresponding to a carrier concentration of 3×10^{18} cm^{-3}. The wafers were degreased in ethanol and acetone and then rinsed with HPLC water before etching. The etch was carried out in a solution of 3 M H_2SO_4 for 3 min to remove the native oxide, followed by a thorough washing with HPLC water. Ohmic contacts were made using Ga−In eutectic.

The orientation of the nanocrystals was determined by X-ray diffraction (XRD) using a high-resolution four-circle diffractometer (Philips X'Pert MRD) with Cu Kα

* To whom correspondence should be addressed. E-mail: jswitzer@umr.edu.
[†] University of Missouri−Rolla.
[‡] Case Western Reserve University.

(1) Petroff, P. M.; Lorke, A.; Imamoglu, A. *Phys. Today* **2001**, *54*, 46.
(2) Leonard, D.; Krishnamurthy, M.; Reaves, C. M.; Denbaars, S. P.; Petroff, P. M. *Appl. Phys. Lett.* **1993**, *63*, 3203.
(3) Eaglesham, D. J.; Cerullo, M. *Phys. Rev. Lett.* **1990**, *64*, 1943.
(4) Mo, Y.-W.; Savage, D. E.; Swartzentruber, B. S.; Lagally, M. G. *Phys. Rev. Lett.* **1990**, *65*, 1020.
(5) Medeiros-Ribeiro, G.; Bratkovski, A. M.; Kamins, T. I.; Ohlberg, D. A. A.; Williams, R. S. *Science* **1998**, *279*, 353.
(6) Alivisatos, A. P. *Science* **1996**, *271*, 933.
(7) Manna, L.; Scher, E. C.; Alivisatos, A. P. *J. Am. Chem. Soc.* **2000**, *122*, 12700.
(8) Puntes, V. F.; Krishnan, K. M.; Alivisatos, A. P. *Science* **2001**, *291*, 2115.
(9) Gou, L.; Murphy, C. J. *Nano Lett.* **2003**, *3*, 231.
(10) Sun, Y.; Xia, Y. *Science* **2002**, *298*, 2176.
(11) Hodes, G. *Electrochemistry of Nanomaterials*; Wiley: New York, 2001.
(12) Switzer, J. A.; Kothari, H. M.; Bohannan, E. W. *J. Phys. Chem. B* **2002**, *106*, 4027.
(13) Switzer, J. A.; Shumsky, M. G.; Bohannan, E. W. *Science* **1999**, *284*, 293.
(14) Bohannan, E. W.; Shumsky, M. G.; Switzer, J. A. *Chem. Mater.* **1999**, *11*, 2289.
(15) Liu, R.; Vertegel, A. A.; Bohannan, E. W.; Sorenson, T. A.; Switzer, J. A. *Chem. Mater.* **2001**, *13*, 508.
(16) Nikiforov, M. P.; Vertegel, A. A.; Shumsky, M. G.; Switzer, J. A. *Adv. Mater.* **2000**, *12*, 1351.
(17) Sorenson, T. A.; Morton, S. A.; Waddill, G. D.; Switzer, J. A. *J. Am. Chem. Soc.* **2002**, *124*, 7604.
(18) Switzer, J. A.; Liu, R.; Bohannan, E. W.; Ernst, F. *J. Phys. Chem. B* **2002**, *106*, 12369.
(19) Lincot, D.; Kampmann, A.; Mokili, B.; Vedel, J.; Cortes, R.; Froment, M. *Appl. Phys. Lett.* **1995**, *67*, 2355.
(20) Pauporte, Th.; Lincot, D. *Appl. Phys. Lett.* **1999**, *75*, 3817.
(21) Liu, R.; Oba, F.; Bohannan, E. W.; Ernst, F.; Switzer, J. A. *Appl. Phys. Lett.* **2003**, *83*, 1944.
(22) Switzer, J. A.; Kothari, H. M.; Poizot, P.; Nakanishi, S.; Bohannan, E. W. *Nature* **2003**, *425*, 490.
(23) De Jongh, P. E.; Vanmaelkelbergh, D.; Kelly, J. J. *Chem. Commun.* **1999**, *12*, 1069.
(24) Snoke, D. *Science* **1996**, *273*, 1351.
(25) Johnsen, K.; Kavoulakis, G. M. *Phys. Rev. Lett.* **2001**, *86*, 858.

10.1021/cm034807c CCC: $25.00
Published on Web 12/02/2003

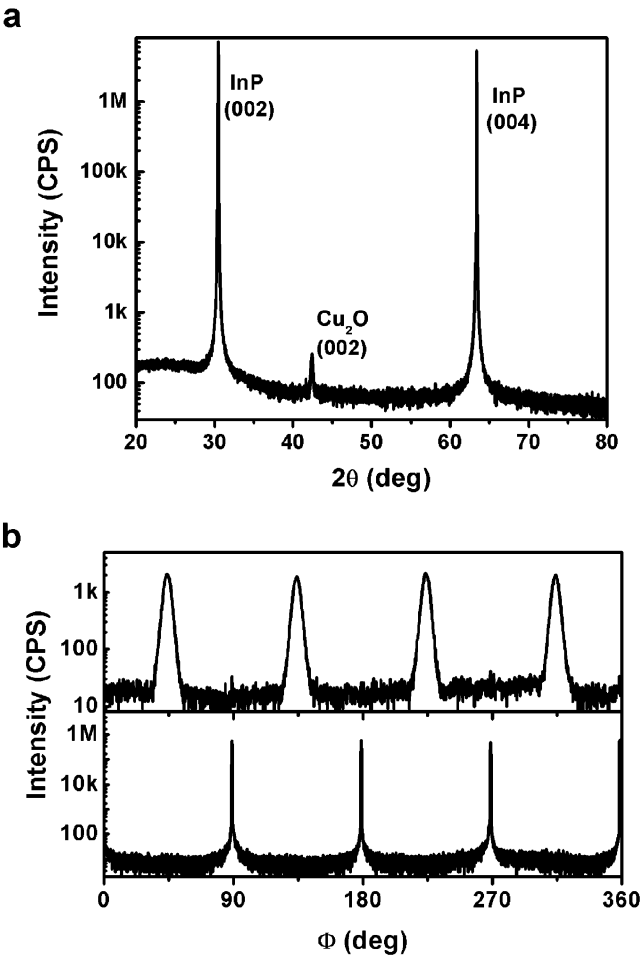

Figure 1. X-ray diffraction results for Cu_2O nanocubes grown from a pH 12 solution on n-InP(001). (a) Bragg-Brentano $\theta-2\theta$ scan of the film. Only the (002) peak for Cu_2O is observed. (b) Azimuthal scans probing the in-plane orientation of the Cu_2O (top) relative to the InP substrate (bottom). The (111) planes of InP at $2\theta = 30.376°$ and Cu_2O at $2\theta = 36.418°$ were brought into the Bragg condition by tilting the sample at $\chi = 54.7°$ and rotating the sample through azimuthal angles, ϕ, of 0−360°. Notice that the Cu_2O has four peaks that are rotated 45° relative to those of InP, consistent with a $Cu_2O(001)[100]$ || $InP(001)[110]$ orientation relationship.

radiation. SEM micrographs were obtained with a Hitachi model S4700 cold field-emission scanning electron microscope. The high-resolution cross-sectional transmission electron microscopy (TEM) image was acquired with a Tecnai F30 ST field-emission gun instrument (FEI), operated at 300 kV.

Results and Discussion. Bragg-Brentano X-ray 2θ scans were used to probe the out-of-plane orientation of the nanocrystals. The X-ray source was Cu $K\alpha_1$ with $\lambda = 0.154056$ nm. The results for the nanocrystals grown at pH 12 (applied charge density of 10 mC/cm^2) are shown in Figure 1a. Only the (002) peak of Cu_2O is observed. The lattice parameter of 0.4269 nm determined for the Cu_2O film is within experimental error of the literature value for that of bulk Cu_2O ($a = 0.4270$ nm),[26] indicating that the majority of the material is completely relaxed. Although only the (002) peak for Cu_2O is observed in Figure 1a, this does not prove the existence of a unique orientation relationship between the Cu_2O and InP. The orientation relationships can be determined by examining the respective azimuthal scans. An azimuthal scan is a two-dimensional cross section at a fixed tilt angle, χ, of a three-dimensional pole figure. Figure 1b shows (111) azimuthal scans for both Cu_2O and InP obtained at $\chi = 54.7°$. This tilt angle corresponds to the angle between the {111} and {001} planes in a cubic crystal system. Rotating the sample through 360° reveals 4-fold symmetry for both the Cu_2O and substrate, consistent with a [001]-oriented crystal. The large lattice mismatch of −27.2% is seen to be accommodated by a 45° rotation of the Cu_2O lattice about the [001] axis relative to the InP substrate. This rotation lowers the lattice mismatch of the corresponding interatomic spacings parallel to the interface from −27.2% to 2.9%. The epitaxial relationship between Cu_2O and substrate can thus be described as $Cu_2O(001)$-[100] || InP(001)[110].

Scanning electron microscopy (SEM) images of Cu_2O grown on InP(001) at pH 9 and 12 are shown in Figure 2. In both cases the electrodeposited materials were examined by XRD prior to SEM imaging and were found to have the $Cu_2O(001)[100]$ || $InP(001)[110]$ epitaxial relationship. Although essentially indistinguishable by XRD, the SEM images reveal fairly dramatic differences in the morphology of the crystallites. Figure 2a shows a plan view of pyramidal nanocrystallites obtained at low surface coverage of Cu_2O grown to a charge density of 10 mC/cm^2 at pH 9. The nanopyramids vary in size from 150 to 200 nm and show a high degree of in-plane ordering consistent with the XRD results. Figure 2b shows a thicker film, grown at pH 9, with a nominal thickness of 0.2 μm. At this point in the growth process the grains have grown larger and coalesced, and the pyramidal structure has become more obvious. Figure 2c shows Cu_2O electrodeposited onto InP(001) to a charge density of 10 mC/cm^2 from a pH 12 solution. In this case, nanocubes of Cu_2O are observed on the surface of the InP. The size measured along the edge of the nanocubes was determined to be 100 ± 15 nm. Figure 2d shows the SEM image of a 0.2-μm-thick Cu_2O film grown at pH 12. The grains have grown larger and coalesced, while the cubelike morphology is maintained.

The difference in the morphology for Cu_2O grown at different pH can be explained in terms of the kinetics of the growth process. The growth rates vary along the different crystallographic directions. We attribute the observed pH dependence of growth rates to the inhibiting effect of solution species such as lactate ion or Cu(II)−lactate complexes which selectively adsorb on various crystal faces. The distribution of these complexes is known to be strongly pH-dependent. The fast growing faces tend to grow out of existence and disappear, while the slower growing faces tend to survive.[27] It has been shown previously that Cu_2O films deposited on polycrystalline substrates grow with a [001] fiber texture at pH 9 and a [111] fiber texture at pH 12.[26] This would suggest that the [001] direction should have the fastest growth rate at pH 9 and the

(26) Golden, T. D.; Shumsky, M. G.; Zhou, Y.; Vanderwerf, R. A.; Van Leeuwen, R. A.; Switzer, J. A. *Chem. Mater.* **1996**, *8*, 2499.

(27) Budevski, E.; Staikov, G.; Lorenz, W. J. *Electrochemical Phase Formation and Growth*; VCH: New York, 1996.

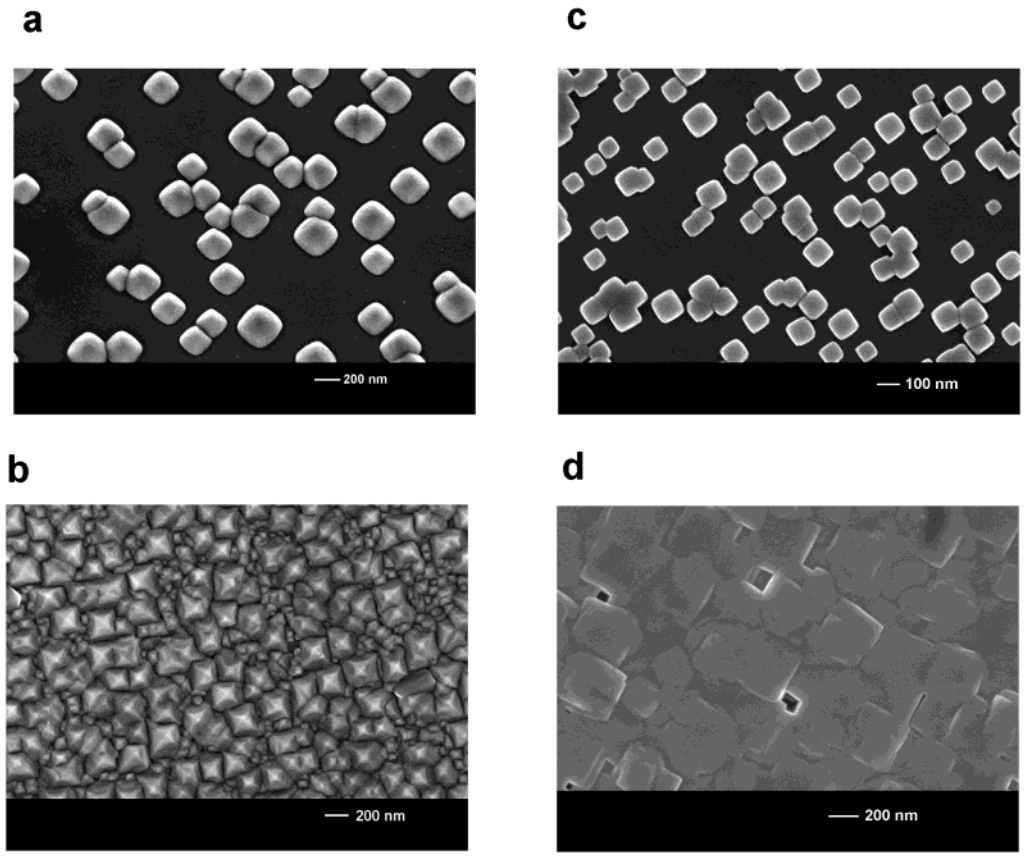

Figure 2. Scanning electron microscope (SEM) images of the epitaxial Cu_2O nanocrystals and films on n-InP(001). (a) Cu_2O nanopyramids (10 mC/cm^2) grown at pH 9; (b) 0.2-μm-thick Cu_2O film grown at pH 9; (c) Cu_2O nanocubes (10 mC/cm^2) grown at pH 12; (d) 0.2-μm-thick Cu_2O film grown at pH 12.

Table 1. Exchange Current Densities for the Deposition of Cu_2O on the Three Low Index Faces of Au at pH 9 and pH 12[12]

	J_0 ($\times 10^{-5}$ A cm^{-2})	
orientation	pH 9	pH 12
[100]	7.3 ± 0.4	3.0 ± 0.4
[110]	4.1 ± 0.4	10.5 ± 0.4
[111]	2.9 ± 0.3	8.5 ± 0.5

[111] direction should have the fastest growth rate at pH 12.

The growth rate along different crystallographic directions has been determined through use of the low overpotential linear approximation of the Butler−Volmer equation on the low index faces of Au in both the pH 9 and pH 12 solutions.[12] The measured exchange current densities are summarized in Table 1. In the case of pH 9, [111] is the slowest growth direction. This is consistent with the pyramidal crystallites observed at pH 9. According to this kinetic argument, the sloping sides of the pyramids are the {111} planes that grow at a slow rate so that they are observed in the SEM images. The flattened tops of the pyramidal crystallites are (001) planes, which do not predominate due to the fast growth along the [001] direction. In the case of pH 12, the slowest growth direction is [001], with growth rates along the [110] and [111] directions being approximately 3 times faster. Once again the faster growing faces tend to grow out of existence, leaving behind the slow growing {001} faces, leading to the observed cubelike morphology.

The Cu_2O/InP interface for the nanocubes formed at pH 12 was studied by cross-sectional transmission electron microscopy (TEM). Figure 3a shows a conventional TEM bright-field image, obtained with a Philips CM20ST operated at 200 kV. The image reveals that individual Cu_2O nanocubes are on top of the InP substrate. There is an interlayer of a different, less scattering material that separates the Cu_2O and InP layers. The selected-area diffraction pattern is shown in the insets of Figure 2a. This was taken from an area that includes a Cu_2O cube and a part of the substrate. Some spots were connected with lines to clarify the orientation relationship: the square and rhombus show the patterns from the Cu_2O and InP, respectively. The viewing direction corresponds to [100] in Cu_2O and [110] in InP, and the [001] normal of the InP corresponds to the [001] direction in Cu_2O. These electron diffraction patterns are consistent with the orientation relationship determined by XRD. Figure 3b shows a high-resolution TEM (HRTEM) image of the interface, obtained with a Tecnai F30 ST field-emission gun instrument (FEI), operated at 300 kV. The image confirms the epitaxial orientation relationship indicated by the X-ray and electron diffraction patterns. It also shows that the interlayer is 5−10 nm thick. The brighter appearance in Figure 3a and the speckle pattern of the interlayer in the HRTEM image of Figure 3b both suggest that the interlayer is amorphous. The amorphous layer was also observed previously in the bulk Cu_2O epitaxial film on InP(100).[21] EDS analysis shows that the amorphous layer is an oxygen-rich layer and is a

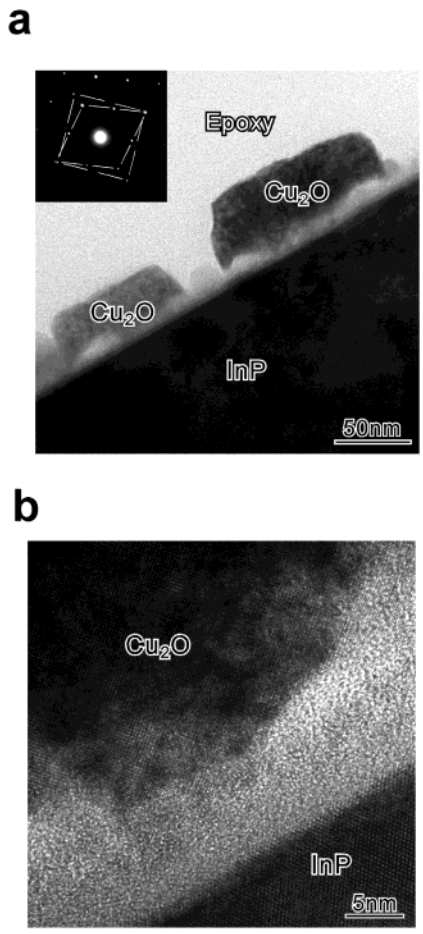

Figure 3. Cross-sectional transmission electron microscopy (TEM) images of the interface between the Cu_2O nanocubes and the InP substrate. (a) Conventional TEM bright-field image, showing that the two materials are separated by an interlayer of a different less-scattering material. The diffraction patterns shown in the insets indicate that the viewing direction corresponds to [100] in the Cu_2O and [110] in the InP and that the [001] normal of the InP substrate corresponds to a [001] direction in the Cu_2O. (b) High-resolution TEM image of the Cu_2O/InP interface. The image confirms the orientation relationship indicated by the X-ray and electron diffraction patterns. The image also shows that the interlayer is 5−10 nm thick and is amorphous.

mixture of In, P, Cu, and O. The InP surface is known to be ordered after H_2SO_4 etching. Yao and Itaya have observed an ordered surface by in situ STM that is consistent with ideal (1 × 1) termination of the bulk structure,[28] while Liu et al. have determined by X-ray diffraction that the surface may be crystalline $InPO_4 \cdot xH_2O$ after H_2SO_4 etching.[29] The amorphous layer in our study may have resulted from a postdeposition reaction between Cu_2O and either InP or $InPO_4 \cdot xH_2O$. Enhanced reactivity of materials is often observed at the interface between two dissimilar materials. Using soft X-ray photoemission, Spicer et al.[30,31] have observed that Cu metal reacts with InP, producing copper-containing phosphides and metallic In. More work needs to be done to identify the origin of this amorphous layer and to understand how the Cu_2O can maintain registry with the substrate despite the amorphous interlayer.

Here, we have shown that ordered Cu_2O nanocrystals can be grown on n-InP(001) using electrodeposition. The growth kinetics can be controlled by the pH of the deposition solution, leading to a pyramidal morphology at pH 9 and a cubelike morphology at pH 12. In addition to the benefits of being able to produce these nanoparticles, control of the growth kinetics can be used to select the exposed planes of a material, which may prove useful in the production of heterogeneous catalysts.

Acknowledgment. This work was supported by NSF Grants CHE-0243424, DMR-0071365, and DMR-0076338, the Department of Energy, the University of Missouri Research Board, and the Foundation for Chemical Research. The Case School of Engineering and the Case Alumni Society are gratefully acknowledged for financial support of this work. F.O. is supported by a Grant-in-Aid for JSPS Fellows from the Ministry of Education, Culture, Sports, Science and Technology of Japan.

CM034807C

(28) Yao, H.; Itaya, K. *J. Electrochem. Soc.* **1998**, *145*, 3090.
(29) Liu, H. C.; Tsai, S. H.; Hsu, J. W.; Shih, H. C. *J. Electrochem. Soc.* **1999**, *146*, 3510.
(30) Kendelewicz, T.; Petro, W. G.; Lindau, I.; Spicer, W. E. *J. Vac. Sci. Technol. B* **1984**, *2*, 453.
(31) Cao, R.; Miyano, K.; Kendelewicz, T.; Lindau, I.; Spicer, W. E. *Appl. Phys. Lett.* **1988**, *53*, 210.